Biotechnology & Biotechnological Equipment

ISSN: (Print) (Online) Journal homepage: https://www.tandfonline.com/loi/tbeq20

Exploration of two major boron transport genes *BOR1* and *NIP5;1* in the genomes of different plants

Ibrahim Ilker Ozyigit, Ertugrul Filiz, Ibrahim Adnan Saracoglu & Sedat Karadeniz

To cite this article: Ibrahim Ilker Ozyigit, Ertugrul Filiz, Ibrahim Adnan Saracoglu & Sedat Karadeniz (2020) Exploration of two major boron transport genes *BOR1* and *NIP5;1* in the genomes of different plants, Biotechnology & Biotechnological Equipment, 34:1, 455-468, DOI: 10.1080/13102818.2020.1773311

To link to this article: https://doi.org/10.1080/13102818.2020.1773311

BIOTECHNOLOGY & BIOTECHNOLOGICAL EQUIPMENT
2020, VOL. 34, NO. 1, 455–468
https://doi.org/10.1080/13102818.2020.1773311

Exploration of two major boron transport genes *BOR1* and *NIP5;1* in the genomes of different plants

Ibrahim Ilker Ozyigit [a,b], Ertugrul Filiz [c], Ibrahim Adnan Saracoglu [d,e] and Sedat Karadeniz [a]

[a]Department of Biology, Faculty of Science and Arts, Marmara University, Goztepe, Istanbul, Turkey; [b]Department of Biology, Faculty of Science, Kyrgyz-Turkish Manas University, Bishkek, Kyrgyzstan; [c]Department of Crop and Animal Production, Cilimli Vocational School, Duzce University, Duzce, Turkey; [d]Department of Chemistry, Faculty of Science and Arts, Marmara University, Goztepe, Istanbul, Turkey; [e]Presidency of the Republic of Turkey, Ankara, Turkey

ABSTRACT

Boron (B) is an essential plant micronutrient but studies regarding its transport are still limited to a few plants. This work identified two major B transport sequences in plants, NIP5;1 boric acid channel protein and BOR1 transporter. 80 *BOR1* and 34 *NIP5;1* homologs were identified in 18 different plant genomes. BOR1 homologs had a HCO3-transporter domain, 649–737 amino-acid residues with mainly basic nature, putative 8–11 transmembrane domains (TMDs) and 11–13 exons. NIP5;1 homologs had a MIP family domain, 294–311 amino-acid residues with basic nature, 5–6 putative TMDs and 3–5 exons. Tyrosine-based motif, acidic di-leucine motif and lysine residue, reported for polarity, vacuolar sorting and B-dependent degradation, were identified in BOR1 homologs. Two NPA motifs and an ar/R selectivity filter with AIGR residues, reportedly essential in B transport, were also found in NIP5;1 homologs. Two NPA motifs in AtNIP5;1 and OsNIP3;1 homologs were NPS and NPV, whereas in sequences homologous to AtNIP6;1 were NPA/V. Besides, ar/R selectivity filters were identified with A(N/S/T)IGR residues in NIP5;1 and NIP3;1 homologs. The BOR1 and NIP5;1 model structures were mainly conserved. Under different perturbations, *Arabidopsis thaliana NIP5;1* and *NIP6;1* genes demonstrated similar expression patterns although they act in different tissues, suggesting a common regulatory mechanism, whereas *BOR1* showed a different expression pattern. *BOR1* was substantially expressed in primary root, radicle and flower; *NIP5;1* in primary root and roots, and *NIP6;1* in petiole. *NIP5;1, 6;1* and *BOR1* expression in other plant organs implied their involvement in different pathways in addition to B uptake and its mobilization.

ARTICLE HISTORY
Received 9 September 2019
Accepted 19 May 2020

KEYWORDS
Boric acid; orthologue; paralog; homolog; motif; selectivity filter

Introduction

Boron (B) is an essential micronutrient for plant life cycle and its deficiency or toxicity can cause significant reductions in crop yield and quality [1,2]. It is involved in many metabolic processes, including control of cell wall porosity and tensile strength [3,4], regulation of membrane potential and permeability [5,6], cytoskeleton polymerization [7], nitrogen and ammonium assimilation [8,9], quantitative and qualitative changes of phenolic compounds [10,11] and cellular signaling [12]. In soil solution, it is present as borate or boric acid ($B(OH)_3$) but the latter is the most accepted form by plants. Based on its availability, boric acid can be taken up by three different mechanisms; *via* diffusion, by major intrinsic proteins (MIP) and by BOR transporters [13,14]. Passive diffusion and MIP transport are employed under the B-sufficient conditions, whereas BOR transporters take role in the B-deficient conditions [15]. In model *Arabidopsis thaliana*, two transport molecules NIP5;1 and BOR1 have been reported in the B transport [14].

NIP5;1 is a boric acid channel in the MIP family, and it is localized to the plasma membranes of root cap and epidermal cells with outside/soil-facing polarity [16,17]. It was significantly upregulated in the B-deficient roots [18] and from the same family NIP6;1 was also reported to be involved in B distribution but in shoots [14]. The members of MIP/aquaporin family were characterized with six putative transmembrane domains (TMDs) and an Asn-Pro-Ala/Ser/Val (NPA) motif signature [19].

CONTACT Ibrahim Ilker Ozyigit ilker.ozyigit@manas.edu.kg; Ertugrul Filiz ertugrulfiliz@gmail.com
Supplemental data for this article is available online at https://doi.org/10.1080/13102818.2020.1773311.

BOR1 transporter was first identified in the B-deficient *A. thaliana* roots. The *AtBOR1* gene includes 12 exons encoding a protein of 704 amino-acid residues with 10 putative TMDs. In addition, six other *A. thaliana* sequences AtBOR2-7 were also reported to show similarities to AtBOR1 [20]. In rice, NIP3;1 and BOR1 are involved in the B uptake under B-deficiency [20,21] and they also show high similarities to the AtNIP5;1 and AtBOR1 respectively [22]. In grapevine, *VvBOR1*, an *AtBOR1* grapevine orthologue, encodes a 720 amino acid residue protein in the plasma membranes [23]. Moreover, functional BOR1 homologs have also been characterized in some other species such as *Saccharomyces cerevisiae* [24], *Eucalyptus* sp. [25] and *Brassica napus* [26]. Furthermore, maize mutant *tls1* was reported to encode a NIP3;1 protein, an AtNIP5;1 orthologue and similarly maize mutant *rte* was demonstrated to encode a B transporter homologous to AtBOR1 with some vegetative and inflorescence/reproductive defects similar to B-deficiency [27–29].

In the light of the above knowledge, B transport molecules NIP5;1 and BOR1 stood out as significant candidates from agricultural perspective to ameliorate the effects of B-deficiency/toxicity and improve the B tolerance in plants. So, this work identified the homologs of these two molecules in the genomes of 18 different plant species, investigated them at primary, secondary and tertiary structural levels, and evaluated the expression profiles under different perturbations and in different plant tissues/organs.

Materials and methods

Retrieval of boron transport sequences

Two functionally characterized B transport sequences, a boric acid channel AtNIP5-1 (Q9SV84.1) and a BOR transporter AtBOR1 (Q8VYR7.1) were obtained from UniProtKB/Swiss-Prot database of NCBI [30]. These sequences were queried as references in proteome datasets of 18 selected plant species in Phytozome [31] database with an $\leq e^{-98}$ threshold, except *Chlamydomonas reinhardtii* ($\leq e^{-15}$). Studied plants included *Arabidopsis thaliana, Brachypodium distachyon, Brassica rapa, C. reinhardtii, Cucumis sativus, Eucalyptus grandis, Glycine max, Gossypium raimondii, Medicago truncatula, Oryza sativa, Phaseolus vulgaris, Physcomitrella patens, Populus trichocarpa, Prunus persica, Solanum lycopersicum, Sorghum bicolor, Vitis vinifera* and *Zea mays*. Then, genomic, transcript, coding and peptide sequences of those identified B transporters were retrieved for further bioinformatics analyses.

Analysis of boron transport sequences

Physicochemical properties of sequences including sequence length, molecular weight and isoelectric point were calculated using ProtParam tool [32]. Subcellular localizations were predicted by CELLO server [33]. Protein domain families were checked in Pfam database [34]. Exon/intron organizations of genes were analyzed in GSDS 2.0 server [35]. TMDs were predicted using TMHMM server [36]. Conserved motif sequences were predicted using MEME suite [37] with parameters: max motif number, 5 and min-max motif width, 6–50. Protein sequences were aligned by ClustalW [38] and edited by BioEdit Sequence Alignment Editor [39]. Phylogenetic trees were constructed using MEGA 5 [40] with maximum likelihood (ML) method for 1000 bootstraps and visualized using FigTree [41]. 3 D models of protein sequences were predicted by Phyre^2 server [42] and visualized by using Pymol [43]. Models were validated with Ramachandran analysis [44]. Secondary structural features of models were analyzed using SOPMA server [45]. Expression profiles of B transport genes *BOR1*, *NIP5;1* and *NIP6;1* were investigated using Genevestigator platform in *A. thaliana* [46].

Results and discussion

Sequence analysis of B transporters

Using a channel protein NIP5;1 and a transporter BOR1 sequence from *A. thaliana*, a total of 114 B transport genes, including 80 *BOR1* (Table 1) and 34 *NIP5;1* (Table 2) homologs were identified in the genomes of 18 different plant species by homology search. Identified genes were distributed as per species, *C. reinhardtii* and *P. patens* (two genes each), *B. distachyon*, *C. sativus*, *O. sativa*, *P. persica*, *S. lycopersicum*, *Z. mays* and *S. bicolor* (four genes each), *P. vulgaris* (seven genes), *E. grandis*, *M. truncatula* and *V. vinifera* (eight genes each), *A. thaliana*, *B. rapa* and *G. raimondii* (nine genes each), *G. max* (11 genes) and *P. trichocarpa* (13 genes). All BOR1 homologs were characterized with a HCO3-transporter family (PF00955) domain. *BOR1* genes possessed 11–13 exons encoding proteins of 649–737 amino acid residues with 73.2–81.4 kDa molecular weight and 6.27–9.37 *pI* value, except *C. reinhardtii* (Table 1). *C. reinhardtii* had a 1032-residue protein with 104 kDa molecular weight. BOR1 homologs were also predicted to localize in the plasma membranes with putative 8–11 TMDs. Earlier works reported that the *A. thaliana BOR1* gene has 12 exons encoding a polypeptide of 704 amino-acid residues with 10 putative TMDs and localized to the

Table 1. Putative BOR1 homologs in 18 different plant species and their gene/protein features.

Gene ID (Phytozome)	NCBI protein accession[a]	Product	Homolog/ E-value[b]	Exon no.	Protein length	MW (kDa)	*pI*	TMD no.
AT2G47160	Q8VYR7.1	Probable boron transporter 1	**AtBOR1/0.0**	12	704	78.6	8.86	10
AT3G62270	Q9M1P7.1	Probable boron transporter 2	**AtBOR2/0.0**	12	703	78.6	8.73	10
AT3G06450	Q93Z13.1	Probable boron transporter 3	**AtBOR3/0.0**	12	732	80.7	8.87	8
AT1G15460	Q9XI23.1	Probable boron transporter 4	**AtBOR4/0.0**	12	683	76.7	7.59	10
AT1G74810	Q9SSG5.1	Probable boron transporter 5	**AtBOR5/0.0**	13	683	76.7	6.88	8
AT5G25430	Q3E954.2	Probable boron transporter 6	**AtBOR6/0.0**	13	671	75.5	7.63	11
AT4G32510	Q9SUU1.3	Probable boron transporter 7	**AtBOR7/0.0**	11	673	76.2	8.41	11
Bradi4g04420	XP_003579069.1	Boron transporter 1-like	**AtBOR2/0.0**	12	712	79.2	8.88	10
Bradi2g34110	XP_003568821.1	Boron transporter 4-like	**AtBOR4/0.0**	13	678	76.6	6.82	10
Bradi2g04690	XP_003569518.2	Boron transporter 4-like	**AtBOR4/0.0**	13	666	74.4	6.75	11
Brara.D00064	XP_009138732.1	Probable boron transporter 2	**AtBOR2/0.0**	12	707	78.9	8.63	11
Brara.C03154	XP_009134897.1	Probable boron transporter 3	**AtBOR3/0.0**	12	737	81.1	9.15	8
Brara.F01062	XP_009148940.1	Boron transporter 4	**AtBOR4/0.0**	12	682	76.8	8.30	11
Brara.B02140	XP_009128063.1	Boron transporter 4	**AtBOR4/0.0**	13	683	76.3	6.91	11
Brara.F02740	XP_009151072.1	Probable boron transporter 6	**AtBOR6/0.0**	12	672	75.7	7.26	11
Brara.A00544	XP_009125916.1	Probable boron transporter 7	**AtBOR7/0.0**	12	675	75.8	7.24	10
Cre10.g443900	XP_001690501.1	Borate transporter	**AtBOR1/8e-110**	13	1032	104.0	7.00	9
Cucsa.192570	XP_004151220.1	Probable boron transporter 2-like	**AtBOR2/0.0**	12	717	79.6	8.79	10
Cucsa.098470	XP_004152479.1	Probable boron transporter 2-like	**AtBOR2/0.0**	12	717	80.3	9.07	10
Cucsa.300580	XP_004151241.1	Boron transporter 4-like	**AtBOR4/0.0**	12	661	74.6	7.99	8
Eucgr.H00896	XP_010069747.1	Boron transporter 1-like isoform X2	**AtBOR1/0.0**	12	716	79.3	8.94	11
Eucgr.H04094	XP_010024845.1	Probable boron transporter 2	**AtBOR2/0.0**	12	706	78.4	9.37	10
Eucgr.B00302	XP_010027612.1	Boron transporter 1-like	**AtBOR2/0.0**	12	709	79.3	9.05	10
Eucgr.J03035	XP_010033916.1	Boron transporter 4	**AtBOR4/0.0**	13	669	75.5	8.05	11
Eucgr.C04162	XP_010049957.1	Boron transporter 4-like isoform X1	**AtBOR4/0.0**	13	668	74.9	6.43	11
Eucgr.C02816	XP_010048993.1	Probable boron transporter 7	**AtBOR4/0.0**	13	668	75.3	8.12	10
Glyma.06G181900	XP_003527015.1	Boron transporter 1-like isoform X1	**AtBOR2/0.0**	12	723	80.6	9.21	9
Glyma.04G184000	XP_003523082.1	Boron transporter 1-like isoform X1	**AtBOR2/0.0**	12	720	80.2	9.17	9
Glyma.19G219500	XP_003554567.1	Boron transporter 1-like	**AtBOR2/0.0**	12	723	80.6	8.92	9
Glyma.03G222300	XP_003521605.1	Boron transporter 1-like isoform 1	**AtBOR2/0.0**	12	723	80.7	8.84	9
Glyma.09G031400	XP_003533117.1	Probable boron transporter 2-like isoform X1	**AtBOR2/0.0**	12	708	78.7	9.05	9
Glyma.15G011200	XP_003546177.1	Boron transporter 4-like isoform X1	**AtBOR4/0.0**	13	669	75.2	7.20	9
Glyma.04G069500	XP_006578164.1	Boron transporter 4-like	**AtBOR7/0.0**	12	662	74.3	7.55	10
Glyma.17G207700	XP_006601135.1	Probable boron transporter 6-like	**AtBOR6/0.0**	12	663	74.5	8.20	12
Gorai.005G070200	KHG10152.1*	Boron transporter 1-like protein	**AtBOR1/0.0**	12	716	80.1	8.66	10
Gorai.005G135900	KHG05664.1*	Boron transporter 1-like protein	**AtBOR2/0.0**	12	715	79.3	8.89	9
Gorai.008G137000	KHG13958.1*	Boron transporter 1-like protein	**AtBOR1/0.0**	11	710	79.2	8.63	10
Gorai.006G266200	KHG11152.1*	putative boron transporter 2 -like protein	**AtBOR2/0.0**	12	712	79.4	8.75	8
Gorai.004G146300	KHG23411.1*	putative boron transporter 2 -like protein	**AtBOR2/0.0**	12	717	79.7	8.90	9
Gorai.011G205300	————————	————————	**AtBOR4/0.0**	12	662	74.9	8.77	9
Gorai.009G010600	————————	————————	**AtBOR4/0.0**	13	673	76.3	7.91	9
Medtr2g032690	XP_003594631.1	Boron transporter	**AtBOR1/0.0**	13	708	79.7	8.60	10
Medtr7g110000	XP_003626013.1	Boron transporter	**AtBOR2/0.0**	12	724	80.8	8.99	10
Medtr3g077670	XP_003601253.1	Boron transporter	**AtBOR2/0.0**	12	703	78.0	8.44	9
Medtr0459s0020	KEH15890.1	Boron transporter-like protein	**AtBOR4/0.0**	13	659	74.3	8.23	10
Medtr3g107730	AES73690.2	Boron transporter-like protein	**AtBOR7/0.0**	11	678	76.5	7.86	10
LOC_Os12g37840	AAQ02664.1	Boron transporter	**AtBOR2/0.0**	12	711	79.3	9.07	9
LOC_Os01g08020	ABD78950.1	Boron transporter	**AtBOR4/0.0**	13	672	75.6	6.33	10
LOC_Os05g08430	ABD78951.1	Boron transporter	**AtBOR5/0.0**	13	677	76.2	8.63	10
Phpat.001G035800	XP_001759676.1	Hypothetical protein	**AtBOR2/0.0**	13	700	77.6	8.16	8

(*continued*)

Table 1. Continued.

Gene ID (Phytozome)	NCBI protein accession[a]	Product	Homolog/ E-value[b]	Exon no.	Protein length	MW (kDa)	*pI*	TMD no.
ppa002139m.g	XP_007225187.1	Hypothetical protein	**AtBOR2/0.0**	12	710	79.1	8.97	10
ppa002104m.g	XP_007221557.1	Hypothetical protein	**AtBOR2/0.0**	12	716	79.3	9.01	9
ppa002100m.g	XP_007210327.1	Hypothetical protein	**AtBOR2/0.0**	12	716	79.9	9.24	10
Potri.002G191000	XP_002301535.1	Anion exchange family protein	**AtBOR2/0.0**	12	731	81.4	9.13	10
Potri.008G100300	XP_002311364.1	Hypothetical protein	**AtBOR2/0.0**	12	712	79.2	9.05	10
Potri.015G077600	XP_002321602.2	Hypothetical protein	**AtBOR2/0.0**	12	720	80.3	9.06	10
Potri.012G081800	XP_006376859.1	Hypothetical protein	**AtBOR2/0.0**	12	720	80.4	8.88	9
Potri.001G174500	XP_002299613.2	Anion exchange family protein	**AtBOR4/0.0**	13	668	75.0	8.32	10
Potri.003G059700	XP_002304164.2	Anion exchange family protein	**AtBOR4/0.0**	13	678	76.7	7.59	10
Potri.006G154700	XP_002309238.2	Hypothetical protein	**AtBOR4/0.0**	13	667	74.2	8.35	8
Potri.006G249800	XP_002308645.1	Hypothetical protein	**AtBOR4/0.0**	11	666	75.2	8.21	10
Potri.018G031700	XP_002324278.1	Hypothetical protein	**AtBOR4/0.0**	11	666	75.2	7.98	8
Phvul.001G215700	XP_007163214.1	Hypothetical protein	**AtBOR2/0.0**	12	723	80.4	8.84	9
Phvul.009G178000	XP_007138070.1	Hypothetical protein	**AtBOR2/0.0**	12	722	80.1	9.18	9
Phvul.005G174400	XP_007150705.1	Hypothetical protein	**AtBOR4/0.0**	13	673	75.4	7.69	9
Phvul.001G053300	XP_007161235.1	Hypothetical protein	**AtBOR6/0.0**	12	649	73.2	6.45	10
Sobic.008G132300	————————	————————	**AtBOR2/0.0**	12	709	79.1	9.19	10
Sobic.009G064200	XP_002440699.1	Hypothetical protein	**AtBOR4/0.0**	13	687	76.7	8.04	9
Sobic.003G047900	XP_002455089.1	Hypothetical protein	**AtBOR4/0.0**	13	663	74.1	6.38	11
Solyc01g079150.2	XP_004229368.1	Boron transporter 1	**AtBOR1/0.0**	12	720	80.4	9.00	10
Solyc06g071500.2	XP_004241498.1	Probable boron transporter 2	**AtBOR2/0.0**	12	720	80.4	9.09	9
GSVIVT01017647001	XP_010649608.1	uncharacterized protein isoform X3	**AtBOR2/0.0**	12	717	80.1	8.97	9
GSVIVT01028186001	XP_010652294.1	Probable boron transporter 2	**AtBOR2/0.0**	12	717	79.8	9.07	10
GSVIVT01007733001	XP_002282501.1	Probable boron transporter 2	**AtBOR2/0.0**	12	720	80.2	8.83	10
GSVIVT01015478001	XP_002281778.2	Boron transporter 4	**AtBOR4/0.0**	13	675	76.4	7.61	8
GSVIVT01017223001	XP_002285279.1	Boron transporter 4	**AtBOR4/0.0**	12	668	75.0	8.46	10
GSVIVT01035800001	XP_002282436.1	Probable boron transporter 7	**AtBOR4/0.0**	13	669	75.3	7.93	10
GRMZM2G082203	NP_001167745.1	Hypothetical protein	**AtBOR2/0.0**	12	702	78.3	9.00	10
GRMZM2G166159	NP_001151747.1	LOC100285382	**AtBOR2/0.0**	12	709	78.9	9.13	10
GRMZM2G051753	XP_008672825.1	Boron transporter-like protein 2 isoform X1	**AtBOR4/0.0**	13	670	74.8	6.27	10

[a]Protein sequences of retrieved genes were p-blasted in NCBI. If a sequence demonstrated ≥95 query cover and identity for a particular protein, that protein accession number was adapted as NCBI accession, with the exception of *C. reinhardtii* since it only has a single entry in NCBI (91% identity and 51% query cover).

[b]Homologs of retrieved genes and how much homology they showed were indicated in this column.

*Since no entry was found for *G. raimondii,* a close species such as *G. arboreum* in the same genus, which has ≥95 query cover and ≥80 identity, was adapted as NCBI accession.

Dash (-) lines indicate that there is no entry found for neither queried species nor its close relative in the same genus.

Table 2. Putative NIP5;1 homologs in 18 different plant species and their gene/protein features.

Gene ID (Phytozome)	NCBI protein accession[a]	Product	Homolog/ E-value[b]	Exon no.	Protein length	MW (kDa)	*pI*	TMD no.
AT4G10380	Q9SV84.1	Probable aquaporin NIP5-1	**AtNIP5;1/0.0**	4	304	31.4	8.65	5
AT1G80760	Q9SAI4.1	Aquaporin NIP6-1	**AtNIP6;1/0.0**	5	305	31.8	8.33	6
Bradi3g30540	XP_003574178.1	Aquaporin NIP3-1	**OsNIP3;1/0.0**	3	301	31.2	9.10	5
Brara.B02894	XP_009128716.1	Probable aquaporin NIP5-1	**AtNIP5;1/0.0**	4	301	31.1	8.66	5
Brara.B02396	XP_009128393.1	Aquaporin NIP6-1-like	**AtNIP6;1/0.0**	5	305	31.8	7.69	6
Brara.C02640	XP_009134192.1	Probable aquaporin NIP5-1	**AtNIP5;1/0.0**	4	301	31.2	8.90	5
Cre12.g549300	XP_001694120.1	Aquaporin, glycerol transport activity	**ZmPIP1;5/ 5e-25**	5	300	31.5	6.51	5
Cucsa.193180	XP_004145889.1	Probable aquaporin NIP5-1-like	**AtNIP5;1/0.0**	4	298	30.8	8.63	5
Eucgr.D02548	XP_010054000.1	Probable aquaporin NIP5-1	**AtNIP5;1/0.0**	4	294	30.6	8.87	5
Eucgr.J03103	XP_010034003.1	Aquaporin NIP6-1	**AtNIP6;1/0.0**	5	298	30.2	8.72	6
Glyma.08G217400	XP_003531732.1	Aquaporin NIP6-1-like	**AtNIP6;1/0.0**	5	306	31.7	9.13	5
Glyma.10G221100	XP_003535560.1	Probable aquaporin NIP5-1-like	**AtNIP5;1/0.0**	4	299	31.1	7.68	5
Glyma.15G003900	XP_003547292.1	Aquaporin NIP6-1-like	**AtNIP6;1/0.0**	3	304	31.2	8.25	6
Gorai.004G126900	KHG22884.1*	Putative aquaporin NIP5-1-like protein	**AtNIP5;1/0.0**	4	298	31.1	8.57	5
Gorai.009G124500	KHG25640.1*	Aquaporin NIP6-1-like protein	**AtNIP6;1/0.0**	5	300	30.9	8.99	6
Medtr2g104940	AAT35231.1	Nodulin 26-like protein	**AtNIP6;1/0.0**	5	310	32.2	8.77	6
Medtr4g006730	XP_003604218.1	Nodulin-like intrinsic protein NIP1-1	**AtNIP6;1/0.0**	5	305	31.6	8.32	6
Medtr1g097840	XP_003592016.1	Aquaporin NIP3-1	**AtNIP5;1/0.0**	4	300	31.0	8.77	5
LOC_Os10g36924	Q0IWF3.2	NOD26-like intrinsic protein 3-1	**OsNIP3;1/0.0**	3	311	31.8	9.08	6
Phpat.015G050300	XP_001779449.1	Hypothetical protein	**AtNIP5;1/0.0**	5	301	31.9	9.22	6
ppa009083m.g	XP_007215732.1	Hypothetical protein	**AtNIP6;1/0.0**	5	307	31.9	8.34	6
Potri.003G180900	XP_002304723.1	Aquaporin NIP6.1 family protein	**AtNIP6;1/0.0**	5	303	31.2	8.60	6
Potri.001G455000	XP_002298990.1	Hypothetical protein	**AtNIP5;1/0.0**	4	299	31.0	8.62	5
Potri.001G046800	XP_002297797.2	Aquaporin NIP6.1 family protein	**AtNIP6;1/0.0**	5	303	31.2	8.28	6
Potri.011G146900	XP_002317642.1	Hypothetical protein	**AtNIP5;1/0.0**	4	300	31.3	8.84	5
Phvul.007G084000	XP_007143584.1	Hypothetical protein	**AtNIP5;1/0.0**	4	299	31.3	8.56	5
Phvul.005G182400	XP_007150811.1	Hypothetical protein	**AtNIP6;1/0.0**	4	303	31.3	8.26	6
Phvul.010G160200	XP_007135806.1	Hypothetical protein	**AtNIP6;1/0.0**	5	301	31.2	8.59	6
Sobic.001G195800	XP_002464380.1	Hypothetical protein	**OsNIP3;1/0.0**	4	301	31.1	9.08	5
Solyc03g117050.2	NP_001289852.1	Aquaporin NIP6-1-like	**AtNIP6;1/0.0**	5	306	31.6	8.34	7
Solyc08g013730.2	NP_001274288.1	Probable aquaporin NIP5-1-like	**AtNIP5;1/0.0**	4	295	30.6	9.06	5
GSVIVT01019729001	XP_002276319.1	Probable aquaporin NIP5-1	**AtNIP5;1/0.0**	4	298	30.6	9.08	5
GSVIVT01034224001	XP_002272988.1	Aquaporin NIP6-1	**AtNIP6;1/0.0**	4	354	37.3	8.28	6
GRMZM2G176209	Q9ATN1.1	Aquaporin NIP3-1	**ZmNIP3;1/0.0**	4	302	31.1	9.22	6

[a]Protein sequences of retrieved genes were p-blasted in NCBI. If a sequence demonstrated ≥95 query cover and identity with a particular protein, that protein accession number was adapted as NCBI accession, with the exception of *P. patens* since it only has a single entry in NCBI (100% identity and 81% query cover).

[b]Homologs of retrieved genes and how much homology they showed were indicated in this column.

*Since no entry was found for *G. raimondii,* a close species such as *G. arboreum* in the same genus, which has ≥95 query cover and identity, was adapted as NCBI accession.

Table 3. Five most conserved motifs in BOR1 and NIP5;1 homologs in 18 different plant species.

	Motif no	Motif width	Motif Sequence	Domain family (Pfam)*
BOR1	1	50	QMAQQKEFNLKKPSSYHYDILLLGFMTLMCGLIGIPPSNGVIPQSPMHTK	HCO3- transporter family
	2	50	IPTSVLWGYFAYMAIDSLPGNQFWERILLLFTAPSRRYKVLEDYHATFVE	HCO3- transporter family
	3	50	FGEQLERDTDGVLTAVQTLASTAICGIIHSIIGGQPLLILGVAEPTVIMY	HCO3- transporter family
	4	50	WTGWVCVWTALLLFLLAIFNACSIINRFTRIAGELFGMLIAMLFMQQAIK	HCO3- transporter family
	5	50	NGMFALVFSFGLLYTALKSRKARSWRYGTGWLRGFIADYGVPLMVVVWTA	Not found
NIP5;1	1	50	HISGAHLNPSLTIAFAALRHFPWKHVPVYIGAQVSASICASFALKGVFHP	Major intrinsic protein
	2	50	FNLMFVVTAVATDTRAVGELAGIAVGATVMLNILIAGPTTGGSMNPVRTL	Major intrinsic protein
	3	50	RKLGAEFVGTFILIFAATATPIVNQKYQGSETLIGNAACAGLAVMIIILS	Not found
	4	41	GPAIAANNYKQIWIYLVAPTLGALCGAGTYTAVKLRDEDDD	Major intrinsic protein
	5	15	PSVSYGQAFALEFII	Not found

*HCO3- transporter family (PF00955), Major intrinsic protein (PF00230).

plasma membrane of pericycle cells [24]. Rice *BOR1* encodes 711 amino-acid residues with putative 10 TMDs localized to the plasma membrane [20]. *VvBOR1*, a grapevine orthologue of *AtBOR1*, encodes a protein of 720 amino acid residues in the plasma membranes [23]. In a different study, maize mutant *rte* was reported to encode a membrane-localized B efflux transporter, which demonstrates high similarity to the AtBOR1 protein [27]. Thus, herein BOR1 homologs showed compliance with findings of the previous works. So, we may report that plant *BOR1* homologs could be characterized with 11–13 exons encoding 649–737 amino-acid residues with a HCO3-transporter family domain and putative 8–11 TMDs.

Besides, homologs of boric acid channel NIP5;1 proteins were characterized with a MIP family (PF00230) domain [47]. *NIP5;1* genes possessed 3–5 exons encoding a protein of 294–311 amino-acid residues with 30.2–32.2 kDa molecular weight and 8.26–9.22 *pI* value, except a *V. vinifera* (GSVIVT01034224001) member with 354 amino-acid residues and 37.3 kDa molecular weight (Table 2). NIP5;1 homologs were predicted to be localized in the plasma membranes with putative 5–6 TMDs. In previous studies, NIP5;1 was reported to be a boric acid channel in the MIP family [18]. It is localized to the plasma membranes of root cap and epidermal cells with outside/soil-facing polarity [17]. MIP members were characterized with six putative TMDs and an NPA motif signature [19]. NIP5;1 sequences were identified in a number of species with common NPA motif, including *Z. mays* (NCBI access: AFW61239; 296 amino acids), *S. lycopersicum* (access: BAO18646; 295 aa), *A. thaliana* (access: AEE82874; 304 aa), *Nicotiana tabacum* (access: AIL50151; 297 aa), *Glycine soja* (access: KHN46385; 299 aa), *Gossypium arboreum* (access: KHG22884; 298 aa), *Lotus japonicus* (access: ABY19373; 302 aa) and *Morus notabilis* (access: EXB56000; 298 aa). Thus, we mention that NIP5;1 homologs in plants could be identified with a MIP family domain, 294–311 residues protein with basic nature, putative 5–6 TMDs, 3–5 exons and a NPA motif.

Conserved motifs in B transport sequences

To figure out the conserved sequences in B transporters, most conserved five motifs were identified in the BOR1 and NIP5;1 homologs (Table 3). In BOR1 homologs, motifs 1–4 were related with the HCO3-transporter (PF00955) family domain, whereas motif 5 did not relate to any protein family. Besides, five motifs were present in all BOR1 sequences. In NIP5;1 homologs, motif 1, 2 and 4 were associated with the MIP family (PF00230) domain, whereas motif 3 and 5 did not relate to any protein family. Except for motifs 3–5 in *C. reinhardtii,* five motifs were conserved in all NIP5;1 sequences. In addition, the width of the identified motifs in both BOR1 and NIP5;1 homologs were relatively long, giving clues about the well conserved nature of B transport sequences in plants (also refer to Supplemental Figures S1 and S2).

To further investigate the protein sequence conservancy, BOR1 and NIP5;1 homologs in 18 plant species were aligned by ClustalW, and identical and similar residues were shaded in black and gray respectively. In aligned BOR1 homologs (Supplemental Figure S1), residues Val (V), Leu (L), Met (M), His (H), Pro (P), Arg (R), Gly (G), Gln (Q), Glu-Gln-Arg (EQR), Gly-Tyr-Phe (GYF), Phe-Thr (FT), Phe-Pro (FP) and Leu-Asp (LD) were found to be fully preserved in sequences of all 18 plant species. It has been reported that three motif sequences such as tyrosine-based motif (YxxM/L; Y/FxxML), acidic di-leucine motif (D/ExxxLL) and lysine residue (N/FKx) are required for polarity and vacuolar sorting in AtBOR1 [17,48–50]. In BOR1 sequences, we have identified two tyrosine-based motifs similar to the sequences identified by Wakuta *et al.* [50]. In first tyrosine-based motif, YxxM signature was present in all AtBOR1 homologs, whereas YxxL was in homologs of AtBOR4-7. However, a second tyrosine-based motif, Y/F/IxxM was present in BOR1 homologs with some

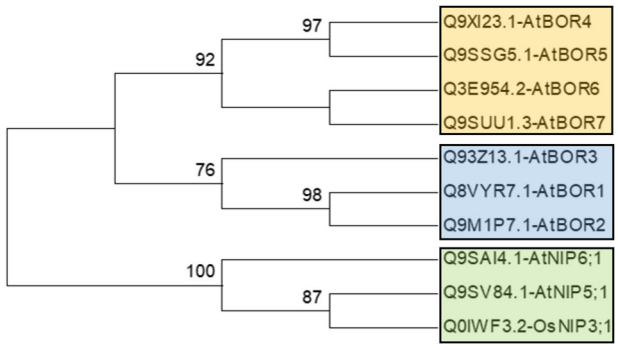

Figure 1. Phylogenetic distribution of known BOR transporter and boric acid channel proteins in *Arabidopsis thaliana* and *Oryza sativa*. Phylogeny was constructed by MEGA 6 using ML method for 1000 bootstraps. This tree is used as benchmark to determine the clustering pattern of studied sequences.

displacements. In addition, acidic di-leucine motif and lysine residue were also identified in BOR1 sequences. Thus, given motifs may also be responsible for polarity and vacuolar sorting in some homologs.

In aligned NIP5;1 homologs (Supplemental Figure S2), residues Ile (I), His (H), Tyr (Y), Gln (Q), Pro (P), Leu (L), Glu (E), Phe (F), Ala (A), Gly (G), Gly-Thr (GT), Trp/Phe-Val/Ile/Leu-Tyr (WVY), Ile-Ser-Gly-Ala-His-Leu/Val-Asn-Pro-Ser/Ala-Leu/Val/Ile-Thr (ISGAHLNPSLT) and Ser-Met/Leu-Asn-Pro-Val/Ala-Arg-Thr/Ser-Leu/Ile-Gly-Pro-Ala-Val/Ile/Leu (SMNPVRTLGPAV) were highly conserved in all aligned sequences. Studies showed that two Asn-Pro-Ala (NPA) motifs and an ar/R selectivity filter are essential in B transport in boric acid channels. NPA motifs were reported to form one of the major constriction pores in MIP proteins [19,51–53]. Hanaoka *et al.* [21] demonstrated that in cereals and eudicots, two NPA motifs such as NPS and NPV were identical among OsNIP3;1 and AtNIP5;1 orthologues. However, two NPA motifs in OsNIP3;1 paralogs such as OsNIP3;2 and 3;5 were NPA, whereas in AtNIP6;1 paralogs were NPA and NPV. In this study, NPA motifs in AtNIP5;1 and OsNIP3;1 homologs were NPS and NPV, whereas in sequences homologous to AtNIP6;1 were NPA and NPV. Besides, an ar/R selectivity filter was also reported to form another constriction region with four residues in boric acid channels [51]. Residues A, I, G and R were shown to be conserved in NIP5;1 and NIP3;1 orthologues in eudicots and major cereals [21]. Herein, similar residues of ar/R selectivity filter in NIP5;1 and NIP3;1 homologs were also identified. Overall indicated that two NPA motifs and an ar/R selectivity filter are also preserved in the studied sequences, showing their essentiality in B transport of boric acid channels. Furthermore, all given motifs in BOR1 and NIP5;1 homologs could be also used as signatures in characterization of B transporter and boric acid channels in other uncharacterized plants.

Phylogenetic distribution of B transport sequences

The BOR1 and NIP5;1 homologs identified in 18 plant species herein were phylogenetically analyzed using MEGA 6 with the ML method. In the phylogenies, sequences were annotated along with their respective homologs in *A. thaliana* or *O. sativa* since B transport sequences in those two species were well characterized. Homology information was used as benchmark to figure out the clustering pattern of the studied sequences. Initially, a preliminary phylogeny was constructed with known B transport sequences of *A. thaliana* and *O. sativa* to have insights about their phylogenetic relationship, thereby the sequence similarities among them (Figure 1).

The phylogenetic tree of BOR1 homologs demonstrated three major clusters (Figure 2), namely group A (blue segment), B (green segment) and C (red segment). Group A included the AtBOR1-3 homologs without any monocot/dicot separation. Besides, the sequences homologous to AtBOR1 and AtBOR2 were clustered more relatedly than AtBOR3. Preliminary phylogeny also corroborated this (Figure 1), in which AtBOR1 and AtBOR2 sequences demonstrated more similarity to each other and were closely related with AtBOR3. Group B included the AtBOR4-7 homologs without any monocot/dicot separation. In addition, AtBOR4 and AtBOR5 homologs in this group were similar to each other more than the homologs of AtBOR6 and AtBOR7. Preliminary phylogeny (Figure 1) also showed similar distribution, thereby explaining the clustering pattern of the sequences in this group. However, group C only included sequences from the lower plants *C. reinhardtii* (green algae) and *P. patens* (moss) although they showed some similarities to AtBOR1 and AtBOR2 respectively. This indicated the presence of a separation between lower and higher plants for BOR1 transporters. Many previous works also made indications similar to the above. Nakagawa *et al.* [20] demonstrated that AtBOR1-3 are more closely related than AtBOR4-7. AtBOR1-3, OsBOR1 and TaBOR1.1-3 sequences were more closely related than AtBOR4-7 and OsBOR2-4 [54]. Pérez-Castro *et al.* [23] reported similar findings for VvBOR1 compared to the *A. thaliana* BOR sequences.

Furthermore, *AtBOR4*, a *BOR1* paralog of *A. thaliana*, demonstrated B transport activity in transgenic lines [55]. It was also suggested that BOR4 could not be degraded in the posttranslational BOR1 system [56].

Figure 2. Phylogenetic distribution of BOR1 homologs in 18 different plants. Sequences were annotated along with respective homologs in *Arabidopsis thaliana*. Homology information is used as benchmark to determine the clustering pattern of the studied sequences. Circular phylogeny was constructed by MEGA 6 with ML method for 1000 bootstraps and visualized by FigTree. Blue, green and red segments respectively represent group A, B and C.

Miwa *et al.* [57] reported that in high B-availability, BOR4-overexpressing plants have more capability to expand their leaves and accumulate chlorophyll in shoot tissues. This suggested that group B members, including AtBOR4-7 homologs could be involved in various metabolic functions. Moreover, three different clades of B transporters were reported by Wakuta *et al.* [50]. Clade I included AtBOR1, 2 and OsBOR1 proteins functioning in B-limited conditions [20,24,57]. Clade II had AtBOR4 and HvBot1 sequences involved in high B tolerance [56,58] and this clade also included OsBOR4, which is required for pollen germination and/or tube elongation [59]. Clade III included PpBOR1 and PpBOR2. In the light of these studies, the distribution of the BOR1 homologs studied here (Figure 2) also made similar indications, in which the AtBOR1-3 homologs were in group A and the AtBOR4-7 homologs in group B, and group C only had lower plants. It was also implied that plants could acquire two types of B transport mechanisms, one for the low B-availability and another for the high B-tolerance conditions.

Phylogeny of NIP5;1 homologs also showed three major clusters (Figure 3), namely group A (blue segment), B (green segment) and C (red segment). Group A included sequences homologues to AtNIP5;1, OsNIP3;1 and ZmNIP3;1 without any monocot/dicot separation, whereas group B only had AtNIP6;1 homologs with dicots. Preliminary phylogeny (Figure 1) indicated that AtNIP5;1 and OsNIP3;1 are more similar to each other and closely related with AtNIP6;1. This also

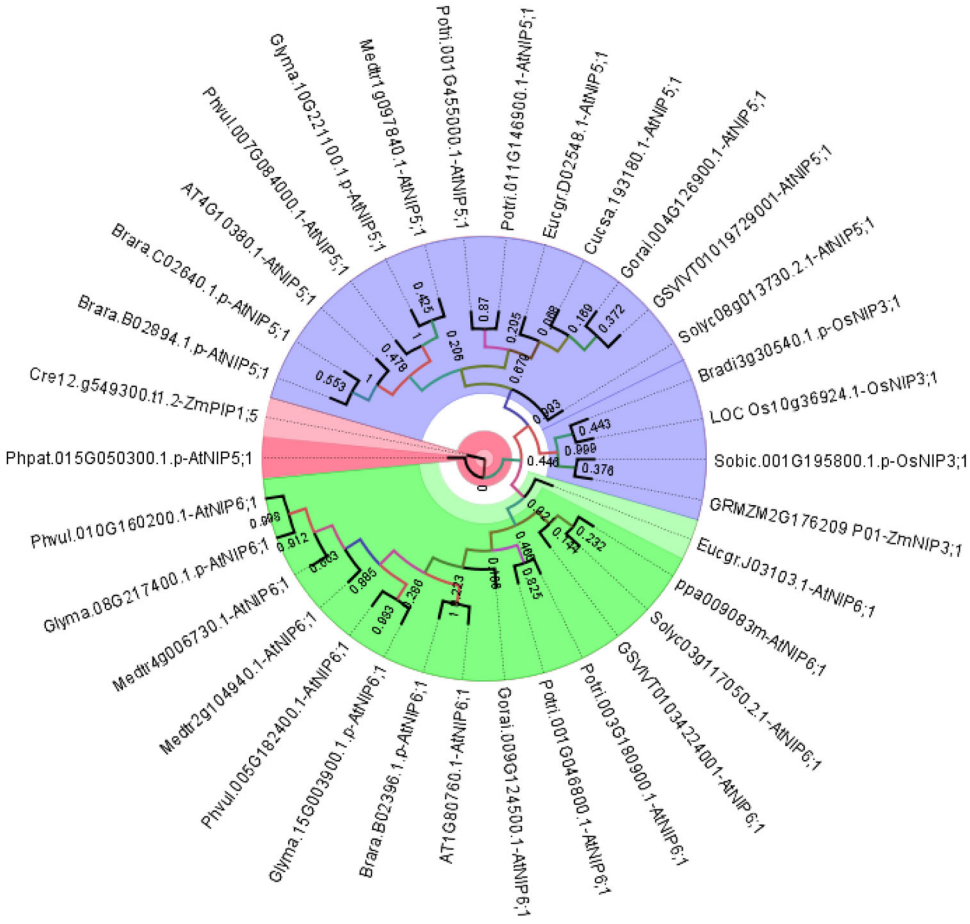

Figure 3. Phylogenetic distribution of NIP5;1 homologs in 18 different plants. Sequences were annotated along with respective homologs in *Arabidopsis thaliana* or *Oryza sativa*. Homology information is used as benchmark determine the clustering pattern of the studied sequences. Circular phylogeny was constructed by MEGA 6 with the ML method for 1000 bootstraps and visualized by FigTree. Blue, green and red segments respectively represent group A, B and C.

explains the sequence distribution in group A and B. In studies, from NIP genes of 10 *O. sativa* and nine *A. thaliana* entries, AtNIP5;1 was more similar to OsNIP3;1 [60]. In a different study, OsNIP3;1 was highly similar to AtNIP5;1 and AtNIP6;1, with 86.2% and 80.0% similarity respectively [21]. Besides, group C only had sequences of lower plants *P. patens* (moss) and *C. reinhardtii* (green algae), indicating a lower/higher plant separation in plants for boric acid channels.

Homology modeling of B transport sequences

Putative 3 D models were constructed by Phyre^2 server using sequences from the selected four plants, including dicots *A. thaliana* and *G. max,* monocot *Z. mays*, and tree species *P. trichocarpa*. BOR1 models were generated from sequences, AT2G47160.1 (*A. thaliana*), Glyma.06G181900.1.p (*G. max*), Potri.002G191000.1 (*P. trichocarpa*) and GRMZM2G082203_P01 (*Z. mays*) based on a single template 4YZF, whereas NIP5;1 models were generated from sequences, AT4G10380.1 (*A. thaliana*), Glyma.10G221100.1.p (*G. max*), Potri.001G455000.1 (*P. trichocarpa*) and GRMZM2G176209_P01 (*Z. mays*) based on the templates 2B6P, 2W2E, 1J4N, 2F2B, 1YMG, 1LDA and 1FX8. Model qualities were validated by Ramachandran plot analysis, the number of allowed residues in BOR1 and NIP5;1 models were calculated as $\geq$88.1 and $\geq$95.3% respectively. This implicated the fairly good structures of the generated models. In BOR1 models, 10 putative TMDs were predicted in 3 D structures, each indicated by a different color (Figure 4). The fully conserved residues identified in the alignment analysis (Supplemental Figure S1) were mapped on the models to show their localization, thereby providing insight into their significance. These residues included Glu-Gln-Arg (EQR) located partially in the TMD9 and loop region, Gly-Tyr-Phe (GYF) in the TMD10, Phe-Thr (FT) in the non-TM helix, Phe-Pro (FP) in the non-TM helix or loop, and Leu-Asp (LD) in the loop. Protein domain analysis demonstrated that these conserved residues approximately correspond to the sites in the HCO3-transporter domain, thereby they may play

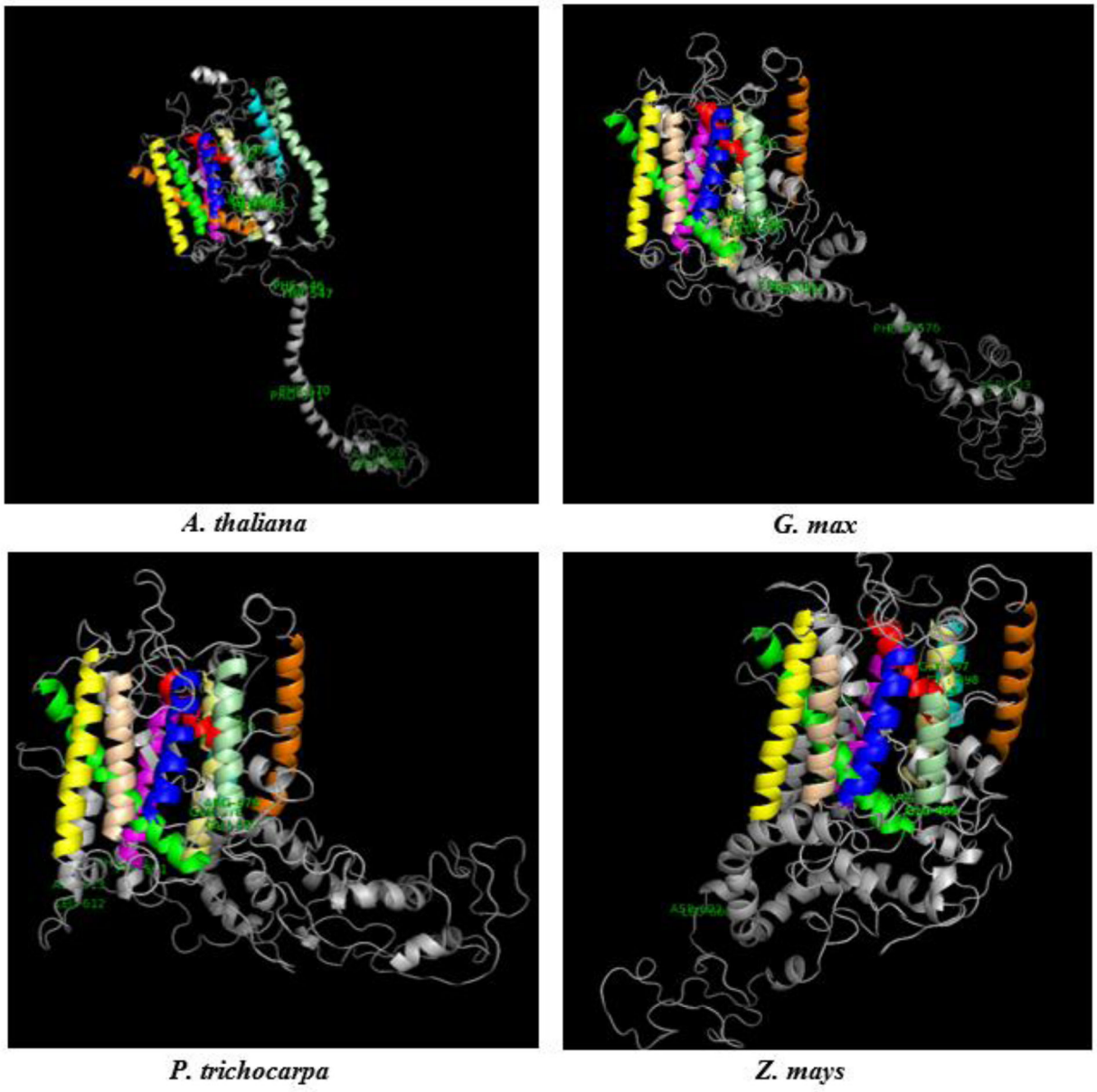

Figure 4. 3 D models of BOR1 transporters from *Arabidopsis thaliana*, *Glycine max*, *Populus trichocarpa* and *Zea mays*. TMDs were specified with different colors, TMD1 with red, TMD2 with blue, TMD3 with yellow, TMD4 with magenta, TMD5 with cyan, TMD6 with orange, TMD7 with green, TMD8 with wheat, TMD9 with pale green, TMD10 with pale yellow, and other structures with gray. Labeled residues show the potential motif signatures identified in alignment analysis.

important role/s in the B transport. In addition, secondary structural features in BOR1s, including α-helix, extended strand, β-turn and random coil respectively, were calculated as 48.15%, 13.64%, 6.68% and 31.53% in *A. thaliana*, 46.33%, 14.25%, 5.26% and 34.16% in *G. max*, 46.92%, 13.95%, 6.57% and 32.56% in *P. trichocarpa*, and 51.00%, 14.25%, 7.41% and 27.35% in *Z. mays*. Despite of some divergences in the secondary structural features and 3 D topologies, the analyzed BOR1 models seemed not to have substantial structural variations.

However, NIP5;1 models were predicted to have six putative TMDs with very similar structures (Figure 5). The fully conserved residues revealed in the alignment analysis (Supplemental Figure S2) were also mapped on the models. They comprised of residues Gly-Thr (GT) located in the TMD1, Trp/Phe-Val/Ile/Leu-Tyr (WVY) in the TMD6, Ile-Ser-Gly-Ala-His-Leu/Val-Asn-Pro-Ser/Ala-Leu/Val/Ile-Thr (ISGAHLNPSLT) in the TMD2, non-TM helix and loop, and Ser-Met/Leu-Asn-Pro-Val/Ala-Arg-Thr/Ser-Leu/Ile-Gly-Pro-Ala-Val/Ile/Leu (SMNPVRTLGPAV) in the non-TM helix and loop. These residues were also found to locate in a region of MIP family domain, thereby they might be inferred with a functional role in the transport of B or other

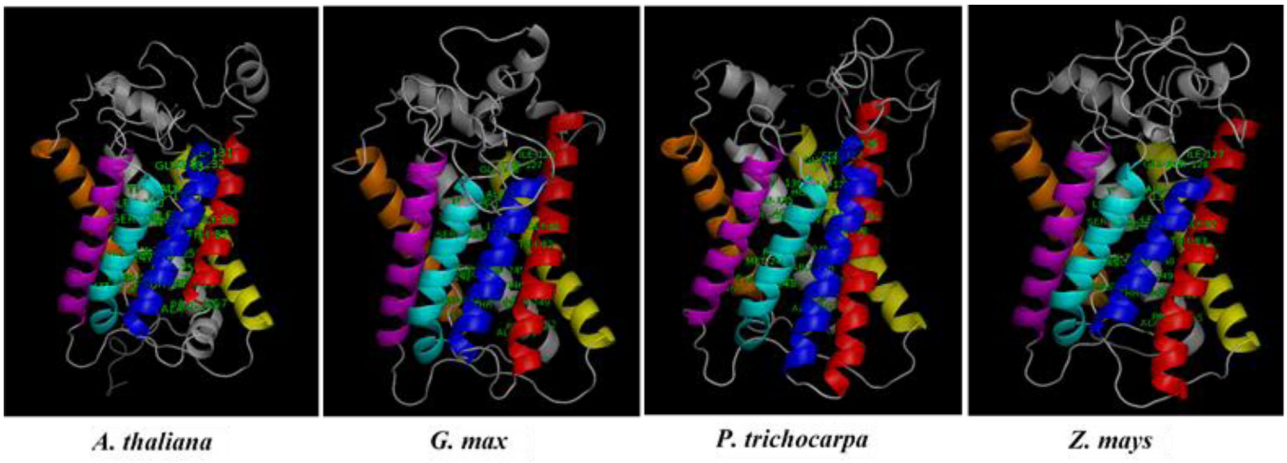

Figure 5. 3 D models of NIP5;1 boric acid channels from *Arabidopsis thaliana*, *Glycine max*, *Populus trichocarpa* and *Zea mays*. TMDs were specified with different colors, TMD1 with red, TMD2 with blue, TMD3 with yellow, TMD4 with magenta, TMD5 with cyan, TMD6 with orange and other structures with gray. Labeled residues show the potential motif signatures identified in alignment analysis.

molecules. In addition, α-helix, extended strand, β-turn and random coil respectively in the NIP5;1 models were calculated as 28.29%, 24.67%, 7.24% and 39.80% in *A. thaliana*, 33.44%, 21.40%, 7.36% and 37.79% in *G. max*, 38.46%, 16.39%, 6.69% and 38.46% in *P. trichocarpa*, and 33.44%, 15.23%, 7.62% and 43.71% in *Z. mays*. Some structural variations were also present in NIP5;1 models; however they were highly conserved compared to the BOR1 models.

Expression profiles of B transport genes

The expression profiles of B transport genes *BOR1*, *NIP5;1* and *NIP6;1* were investigated in the model organism *A. thaliana* under various biotic/abiotic stress conditions (Figure 6(A)) and in different anatomical plant parts (Figure 6(B)) using "Affymetrix *A. thaliana* ATH1 Genome Array" from Genevestigator platform. Seventy-eight different perturbations from biotic, chemical, elicitor, hormone, light, nutrient, photoperiod and other stresses were analyzed with an applied threshold of $-2 \leq x \geq 2$ log2 fold-change. Some studied genes were previously reported for their involvement in B transport. For example, *AtBOR1* gene was mainly expressed in the *A. thaliana* roots under B-deficiency [24,61]. The protein encoded by *NIP5;1* was localized to the plasma membrane of the root cap and epidermal cells, and was significantly upregulated in B-deficient conditions, and the protein encoded by *NIP6;1* was involved in B distribution but in the shoots [14,17,18].

Herein, the expression profiles of *NIP5;1* and *NIP6;1* genes demonstrated similar expression pattern although they were implicated in different tissues. This suggests the presence of a common regulatory mechanism. However, *BOR1* showed a different expression pattern; considering its function in B uptake against the concentration gradient [14], it thus is reasonable to represent a different expression pattern compared to the *NIP5;1* and *NIP6;1*. The given perturbations usually downregulated the *NIP5;1, 6;1* and *BOR1* genes. Especially, some chemical, biotic, deficiency, light, photoperiod and hormone stresses considerably downregulated these genes [61]. However, it seemed that the intensity or the duration of the stress factor rather than its particular type is more effective in exciting the expression of B responsive genes. Moreover, it was interesting that *NIP5;1* and *BOR1* demonstrate different expression patterns although they collaboratively function in B uptake from soil and its loading into xylem under B-deficiency respectively. This implicates the possibility of involvement of other factors in B homeostasis. In plant parts, *NIP5;1, 6;1* and *BOR1* genes were expressed in 44 different anatomical parts in *A. thaliana* at different levels. *BOR1* was substantially expressed in the primary root, radicle and flower; *NIP5;1* showed high expression in the primary root and roots, and *NIP6;1* was in petioles. In addition, all three genes also demonstrated some degree of expression in other plant organs, which may also infer different roles. However, the expression levels of these genes in different plant parts were mainly in agreement with the previous reports, in which *BOR1* and *NIP5;1* were reported to be mainly expressed in B-deficient plant roots, whereas *NIP6;1* was involved in B-distribution in shoots [14,16,18,24]. Thus, the findings from this study suggested the roles of *BOR1* and *NIP5;1* in B uptake and its mobilization, and they also

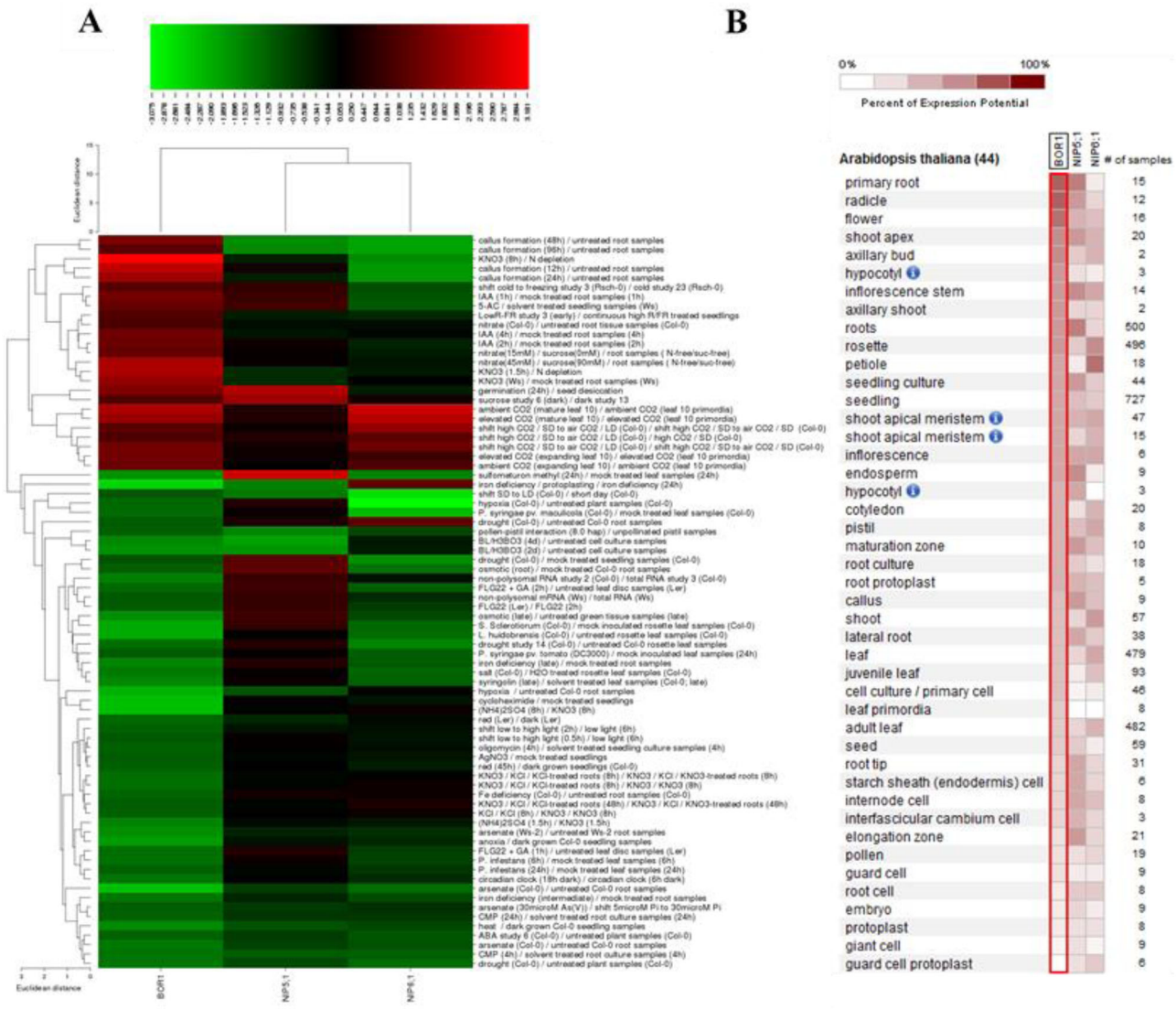

Figure 6. Gene expression profiles (A) and expressed anatomical parts (B) of *Arabidopsis thaliana* B transport genes BOR1, NIP5;1 and NIP6;1 under 78 different perturbations, including biotic, chemical, elicitor, hormone, light, nutrient, photoperiod and other stresses. In expression heatmap (A), conditions (left) and genes (top) with similar expression profiles were hierarchically clustered using Euclidean distance method. Green color indicates the downregulated genes and red color shows the upregulated genes. In anatomical part heatmap (B), blue circles with letter "i" indicate the presence of multiple hierarchical categories for related anatomical parts. For example, seedling > hypocotyl or shoot > hypocotyl.

made implications about the possibility of *NIP5;1, 6;1* and *BOR1* involvement in some other stress responsive mechanisms.

Conclusions

B is an essential plant micronutrient and its deficiency/toxicity leads to significant reductions in crop yield and quality. However, studies about B transporters are limited to some species such as *A. thaliana*, *O. sativa*, *V. vinifera* and *Z. mays*. Thus, the present work identified and characterized 80 BOR1 and 34 NIP5;1 homologs from 18 different plant species. Using known B transport sequences from *A. thaliana* and *O. sativa* at cross-translational way made substantial contributions in interpretation of the identified BOR1 and NIP5;1 homologs. BOR1 and NIP5;1 sequences preserved the earlier reported motif signatures, which inferred roles in polarity and vacuolar sorting, and B transport. Some structural divergences were present in BOR1 and NIP5;1 models but they appeared not to be subjected to substantial changes. Temporal and spatial expression of *A. thaliana NIP5;1, 6;1* and *BOR1* genes implicated their involvement in the stress responsive mechanisms. This work provided knowledge about the primary, secondary and tertiary structures of B transport sequences in various plants, thereby it is thought

to contribute to further manipulations of those genes for molecular or agricultural purposes.

Disclosure statement

No potential conflict of interest was reported by the authors.

ORCID

Ibrahim Ilker Ozyigit http://orcid.org/0000-0002-0825-5951

References

[1] Camacho-Cristóbal JJ, Rexach J, González-Fontes A. Boron in plants: deficiency and toxicity. J Integr Plant Biol. 2008;50(10):1247–1255.

[2] Matthes MS, Robil JM, McSteen P. From element to development: the power of the essential micronutrient boron to shape morphological processes in plants. J Exp Bot. 2020;71(5):1681–1693.

[3] Fleischer A, O'Neill MA, Ehwald R. The pore size of nongraminaceous plant cell walls is rapidly decreased by borate ester cross-linking of the pectic polysaccharide rhamnogalacturonan II. Plant Physiol. 1999; 121(3):829–838.

[4] Ryden P, Sugimoto-Shirasu K, Smith AC, et al. Tensile properties of *Arabidopsis* cell walls depend on both a xyloglucan cross-linked microfibrillar network and rhamnogalacturonan II-borate complexes. Plant Physiol. 2003;132(2):1033–1040.

[5] Ferrol N, Donaire JP. Effect of boron on plasma membrane proton extrusion and redox activity in sunflower cells. Plant Sci. 1992;86(1):41–47.

[6] Wang ZY, Tang YL, Zhang FS, et al. Effect of boron and low temperature on membrane integrity of cucumber leaves. J Plant Nutr. 1999;22(3):543–550.

[7] Bassil E, Hu H, Brown PH. Use of phenylboronic acids to investigate boron function in plants. Possible role of boron in transvacuolar cytoplasmic strands and cell-to-wall adhesion. Plant Physiol. 2004;136(2): 3383–3395.

[8] Shen ZG, Liang YC, Shen K. Effect of boron on the nitrate reductase-activity in oilseed rape plants. J Plant Nutr. 1993;16(7):1229–1239.

[9] Camacho-Cristóbal JJ, González-Fontes A. Boron deficiency decreases plasmalemma H+-ATPase expression and nitrate uptake, and promotes ammonium assimilation into asparagine in tobacco roots. Planta. 2007; 226(2):443–451.

[10] Camacho-Cristóbal JJ, Anzellotti D, González-Fontes A. Changes in phenolic metabolism of tobacco plants during short-term boron deficiency. Plant Physiol Biochem. 2002;40(12):997–1002.

[11] Pasković I, Soldo B, Talhaoui N, et al. Boron foliar application enhances oleuropein level and modulates volatile compound composition in olive leaves. Sci Hortic. 2019;257:108688.

[12] Gonzalez-Fontes A, Rexach J, Navarro-Gochicoa MT, et al. Is boron involved solely in structural roles in vascular plants? Plant Signal Behav. 2008;3(1):24–26.

[13] Aibara I, Hirai T, Kasai K, et al. Boron-dependent translational suppression of the borate exporter BOR1 contributes to the avoidance of boron toxicity. Plant Physiol. 2018;177(2):759–774.

[14] Tanaka M, Fujiwara T. Physiological roles and transport mechanisms of boron: perspectives from plants. Pflugers Arch. 2008;456(4):671–677.

[15] Dannel F, Pfeffer H, Romheld V. Update on boron in higher plant-uptake, primary translocation and compartmentation. Plant Biol. 2002;4(2):193–204.

[16] Sabir F, Gomes S, Loureiro-Dias MC, et al. Molecular and functional characterization of grapevine nips through heterologous expression in aqy-null *Saccharomyces cerevisiae*. IJMS. 2020;21(2):663–682.

[17] Takano J, Tanaka M, Toyoda A, et al. Polar localization and degradation of *Arabidopsis* boron transporters through distinct trafficking pathways. Proc Natl Acad Sci Usa. 2010;107(11):5220–5225.

[18] Takano J, Wada M, Ludewig U, et al. The *Arabidopsis* major intrinsic protein NIP5;1 is essential for efficient boron uptake and plant development under boron limitation. Plant Cell. 2006;18(6):1498–1509.

[19] Kruse E, Uehlein N, Kaldenhoff R. The aquaporins. Genome Biol. 2006;7(2):206–212.

[20] Nakagawa Y, Hanaoka H, Kobayashi M, et al. Cell-type specificity of the expression of OsBOR1, a rice efflux boron transporter gene, is regulated in response to boron availability for efficient boron uptake and xylem loading. Plant Cell. 2007;19(8):2624–2635.

[21] Hanaoka H, Uraguchi S, Takano J, et al. OsNIP3;1, a rice boric acid channel, regulates boron distribution and is essential for growth under boron-deficient conditions. Plant J. 2014;78(5):890–902.

[22] Takano J, Miwa K, Fujiwara T. Boron transport mechanisms: collaboration of channels and transporters. Trends Plant Sci. 2008;13(8):451–457.

[23] Pérez-Castro R, Kasai K, Gainza-Cortés F, et al. VvBOR1, the grapevine ortholog of AtBOR1, encodes an efflux boron transporter that is differentially expressed throughout reproductive development of *Vitis vinifera* L. Plant Cell Physiol. 2012;53(2):485–494.

[24] Takano J, Noguchi K, Yasumori M, et al. *Arabidopsis* boron transporter for xylem loading. Nature. 2002; 420(6913):337–340.

[25] Domingues DS, Leite SMM, Farro APC, et al. Boron transport in Eucalyptus. 2. Identification in silico of a putative boron transporter for xylem loading in eucalypt. Genet Mol Biol. 2005;28(3 suppl):625–629.

[26] Sun J, Shi L, Zhang C, et al. Cloning and characterization of boron transporters in *Brassica napus*. Mol Biol Rep. 2012;39(2):1963–1973.

[27] Chatterjee M, Tabi Z, Galli M, et al. The boron efflux transporter ROTTEN EAR is required for maize inflorescence development and fertility. Plant Cell. 2014; 26(7):2962–2977.

[28] Durbak AR, Phillips KA, Pike S, et al. Transport of boron by the tassel-less1 aquaporin is critical for vegetative and reproductive development in maize. Plant Cell. 2014;26(7):2978–2995.

[29] Leonard A, Holloway B, Guo M, et al. Tassel-less1 encodes a boron channel protein required for

inflorescence development in maize. Plant Cell Physiol. 2014;55(6):1044–1054.
[30] Romiti M. Entrez nucleotide and entrez protein FAQs. Gene. 2010;1:270.
[31] Goodstein DM, Shu S, Howson R, et al. Phytozome: a comparative platform for green plant genomics. Nucleic Acids Res. 2012;40:1178–1186.
[32] Gasteiger E, Hoogland C, Gattiker A, et al. Protein identification and analysis tools on the ExPASy server. In: Walker John M., editor. The proteomics protocols handbook. NJ, USA: Humana Press; 2005. p. 571–607.
[33] Yu CS, Chen YC, Lu CH, et al. Prediction of protein subcellular localization. Proteins. 2006;64(3):643–651.
[34] Sonnhammer EL, Eddy SR, Durbin R. Pfam: a comprehensive database of protein domain families based on seed alignments. Proteins. 1997;28(3):405–420.
[35] Guo AY, Zhu QH, Chen X, et al. GSDS: a gene structure display server. Yi Chuan. 2007;29(8):1023–1026.
[36] Krogh A, Larsson B, von Heijne G, et al. Predicting transmembrane protein topology with a hidden markov model: application to complete genomes. J Mol Biol. 2001;305(3):567–580.
[37] Timothy L, Mikael BB, Buske FA, Frith M, et al. MEME SUITE: tools for motif discovery and searching. Nucleic Acids Res. 2009;37:202–208.
[38] Thompson JD, Higgins DG, Gibson TJ. CLUSTAL W: improving the sensitivity of progressive multiple sequence alignment through sequence weighting, position-specific gap penalties and weight matrix choice. Nucleic Acids Res. 1994;22(22):4673–4680.
[39] Hall T. BioEdit: An important software for molecular biology. GERF Bull Biosci. 2011;2:60–61.
[40] Tamura K, Peterson D, Peterson N, et al. MEGA5: Molecular evolutionary genetics analysis using maximum likelihood, evolutionary distance, and maximum parsimony methods. Mol Biol Evol. 2011;28(10): 2731–2739.
[41] Rambaut A. FigTree. Tree figure drawing tool, v.1.4.0. Institute of Evolutionary Biology, University of Edinburg. 2012. Available from: http://tree.bio.ed.ac.uk/software/figtree/
[42] Kelley LA, Sternberg MJ. Protein structure prediction on the Web: a case study using the Phyre server. Nat Protoc. 2009;4(3):363–371.
[43] DeLano WL. The PyMOL molecular graphics system. San Carlos, CA, USA: DeLano Scientific; 2002.
[44] Lovell SC, Davis IW, Arendall WB, et al. Structure validation by Cα geometry: ϕ, ψ and Cβ deviation. Proteins. 2003;50(3):437–450.
[45] Combet C, Blanchet C, Geourjon C, et al. NPS@: network protein sequence analysis. Trends Biochem Sci. 2000;25(3):147–150.
[46] Hruz T, Laule O, Szabo G, et al. Genevestigator v3: a reference expression database for the meta-analysis of transcriptomes. Adv Intel Soft Compu. 2008;2008: 1–5.
[47] Gómez-Soto D, Galván S, Rosales E, et al. Insights into the role of phytohormones regulating pAtNIP5;1 activity and boron transport in *Arabidopsis thaliana*. Plant Sci. 2019;287:110198
[48] Kasai K, Takano J, Miwa K, et al. High boron-induced ubiquitination regulates vacuolar sorting of the BOR1 borate transporter in *Arabidopsis thaliana*. J Biol Chem. 2011;286(8):6175–6183.
[49] Ou Y, Wu X, Gao Y, et al. Analysis of physiological responses and expression profiling of boron transporter-like genes in response to excess boron in *Populus russkii*. Chemosphere. 2019;224:369–378.
[50] Wakuta S, Mineta K, Amano T, et al. Evolutionary divergence of plant borate exporters and critical amino acid residues for the polar localization and Boron-Dependent Vacuolar Sorting of AtBOR1. Plant Cell Physiol. 2015;56(5):852–862.
[51] de Groot BL, Grubmuller H. Water permeation across biological membranes: mechanism and dynamics of aquaporin-1 and GlpF. Science. 2001;294(5550): 2353–2357.
[52] Gomes D, Agasse A, Thiebaud P, et al. Aquaporins are multifunctional water and solute transporters highly divergent in living organisms. Biochim Biophys Acta. 2009;1788(6):1213–1228.
[53] Zhu Y-X, Yang L, Liu N, et al. Genome-wide identification, structure characterization, and expression pattern profiling of aquaporin gene family in cucumber. BMC Plant Biol. 2019;19(1):345–368.
[54] Leaungthitikanchana S, Fujibe T, Tanaka M, et al. Differential expression of three BOR1 genes corresponding to different genomes in response to boron conditions in hexaploid wheat (*Triticum aestivum* L.). Plant Cell Physiol. 2013;54(7):1056–1063.
[55] Tahghighi H, Erskine W, Bennett RG, et al. Genetic diversity linked to haplotype variation in the world core collection of *Trifolium subterraneum* for boron toxicity tolerance provides valuable markers for pasture breeding. Front Plant Sci. 2019;10:1043–1054.
[56] Miwa K, Takano J, Omori H, Seki M, et al. Plants tolerant of high boron levels. Science. 2007;318(5855): 1417–1417.
[57] Miwa K, Wakuta S, Takada S, et al. Roles of BOR2, a boron exporter, in cross linking of rhamnogalacturonan II and root elongation under boron limitation in *Arabidopsis*. Plant Physiol. 2013;163(4):1699–1709.
[58] Sutton T, Baumann U, Hayes J, et al. Boron-toxicity tolerance in barley arising from efflux transporter amplification. Science. 2007;318(5855):1446–1449.
[59] Tanaka N, Uraguchi S, Saito A, et al. Roles of pollen-specific boron efflux transporter, OsBOR4, in the rice fertilization process. Plant Cell Physiol. 2013;54(12): 2011–2019.
[60] Wallace IS, Choi WG, Roberts DM. The structure, function and regulation of the nodulin 26-like intrinsic protein family of plant aquaglyceroporins. Biochim Biophys Acta. 2006;1758(8):1165–1175.
[61] Luo J, Liang Z, Wu M, et al. Genome-wide identification of BOR genes in poplar and their roles in response to various environmental stimuli. Environ Exp Bot. 2019;164:101–113.